Available online at www.sciencedirect.com
SCIENCE DIRECT®
Journal of Sound and Vibration 272 (2004) 749–771
JOURNAL OF SOUND AND VIBRATION
www.elsevier.com/locate/jsvi

An analytical and experimental investigation of active structural acoustic control of noise transmission through double panel systems

James P. Carneal*, Chris R. Fuller

Vibration and Acoustics Laboratories, Mechanical Engineering Department, Virginia Polytechnic Institute & State University, Blacksburg, VA 24061-0238, USA

Received 9 August 2002; accepted 3 April 2003

Abstract

An analytical and experimental investigation of active control of sound transmission through double panel systems has been performed. The technique used was active structural acoustic control (ASAC) where the control inputs, in the form of piezoelectric actuators, were applied to the structure while the radiating pressure field was minimized. Results verify earlier experimental investigations and indicate the application of control inputs to the radiating panel of the double panel system resulted in greater transmission loss (TL) due to its direct effect on the nature of the structural-acoustic (or radiation) coupling between the radiating panel and the receiving acoustic space. Increased control performance was seen in a double panel system consisting of a stiffer radiating panel due to its lower modal density and also as a result of better impedance matching between the piezoelectric actuator and the radiating plate. In general the results validate the ASAC approach for double panel systems, demonstrating that it is possible to take advantage of double panel system passive behavior to enhance control performance, and provide design guidelines.

1. Introduction

Recent developments in turbofan technology have prompted research into innovative ways of reducing interior noise of aircraft. Ultra high bypass turbofans and unducted fans have increased low frequency noise fields impinging on the exterior of the aircraft fuselage. Traditional methods of low frequency noise reduction require heavy damping material which leads to significant weight penalties, offsetting the performance gains of the turbofans. These factors have prompted the research into applying active control techniques to reduce the interior noise field of a fuselage.

*Corresponding author. Tel.: +1-540-231-3268; fax: +1-540-231-8836.
E-mail address: jcarneal@vt.edu (J.P. Carneal).

0022-460X/$ - see front matter
doi:10.1016/S0022-460X(03)00418-8

This analytical investigation is continuing work previously presented by Carneal and Fuller [1] where the noise transmission path from the exterior of a fuselage through the fuselage skin and the interior trim to the interior noise field was experimentally studied. The experiments used a simplified model of the transmission path; a double panel system mounted in a transmission loss test facility. The incident plate of the double panel system was aluminum that approximated the skin of the aircraft fuselage. The radiating plate of the double panel system was either G10 fiberglass or sandwich board construction which approximated the interior trim of the aircraft. Excitation of the incident plate of the double panel system was provided by a speaker in the source chamber. The radiating plate of the double panel system emitted sound into a reverberant acoustic field in the receiving chamber. Three microphones in the radiated acoustic field provided error signals to a Filtered-X LMS control system. The control signals were input to three piezoelectric actuators mounted on either the incident or radiating plates.

In the experimental investigation [1], it was shown that applying the piezoelectric actuators to the radiating plate of the double panel system has distinct advantages. The application of active structural acoustic control (ASAC) via piezoelectric actuators bonded to the radiating plate of a double panel system will increase the amount of transmission loss through the double panel system and will not increase the vibrational energy of the incident plate. A double panel system with a sandwich board radiating plate (which is relatively stiff) resulted in increased transmission loss due to passive and active effects over one with the G10 fiberglass radiating plate (which is relatively flexible). In addition to these experimental results, another advantage is that the radiating panels can be more easily removed allowing facilitated installation and repair of sensors and actuators.

However, there is a disadvantage that should be mentioned. The application of the control inputs to the interior trim of an aircraft will tend to impart local control of acoustic fields whereas control inputs applied to the fuselage will generally impart global control. This is due to the more continuous, distributed dynamic response of the fuselage structure in the low frequency region. This is mentioned as a separate issue and will be investigated in future work.

For a more detailed literature review, the reader is referred to Ref. [1] also by Carneal and Fuller. This reference compares this approach to other active approaches. In summary, the main advantage of the ASAC approach over the other active approaches applied to double panel systems is the control source which is moved closer to the disturbance to achieve more effective control, the possible use of enclosed active noise sources, etc.

This paper performs an analytical and experimental investigation to further study and verifies the work carried out previously. First, the system description of the analytical model will be discussed followed by a brief overview of the structural and acoustic models. Results are then presented and discussed followed by concluding remarks.

2. Structural and acoustic models

2.1. System description

The application to be studied is the noise transmission path from the exterior of an aircraft to the interior. The structural models of such a system can be approximated by a baffled double

panel arrangement, which consists of an incident plate and a radiating plate coupled by an air cavity. The incident acoustic field in the application is the noise field generated by the propeller of an advanced turboprop engine which can be approximated by an acoustical oblique plane wave. The radiated acoustic field of the double panel system is the interior of an aircraft, which we assume is highly damped and can be approximated by an acoustical free field. These assumptions are necessary to provide a deterministic model of the transmitted power, which can be found by integrating the acoustic pressure over a hemisphere in the free field. Control is provided by piezoelectric actuators mounted on either the incident plate or the radiating plate of the double panel system. The system schematic is presented in Fig. 1.

Dimensions and parameters of this investigation were chosen to be identical to the previous experiments. The incident plate is made of aluminum of dimensions $380 \times 300 \times 1.6$ mm thick. The radiating plate material is either aluminum of the same dimensions as the incident plate (which is relatively flexible) or sandwich board of dimensions $380 \times 300 \times 10.2$ mm thick (which is relatively stiff). Both plates are assumed to be located in a rigid wall whose surfaces are flush with the incident and radiating plates as shown in Fig. 1. The incident and radiating plates are coupled by an air cavity of dimensions 380×300 and 48 mm thick. The double panel system is assumed to

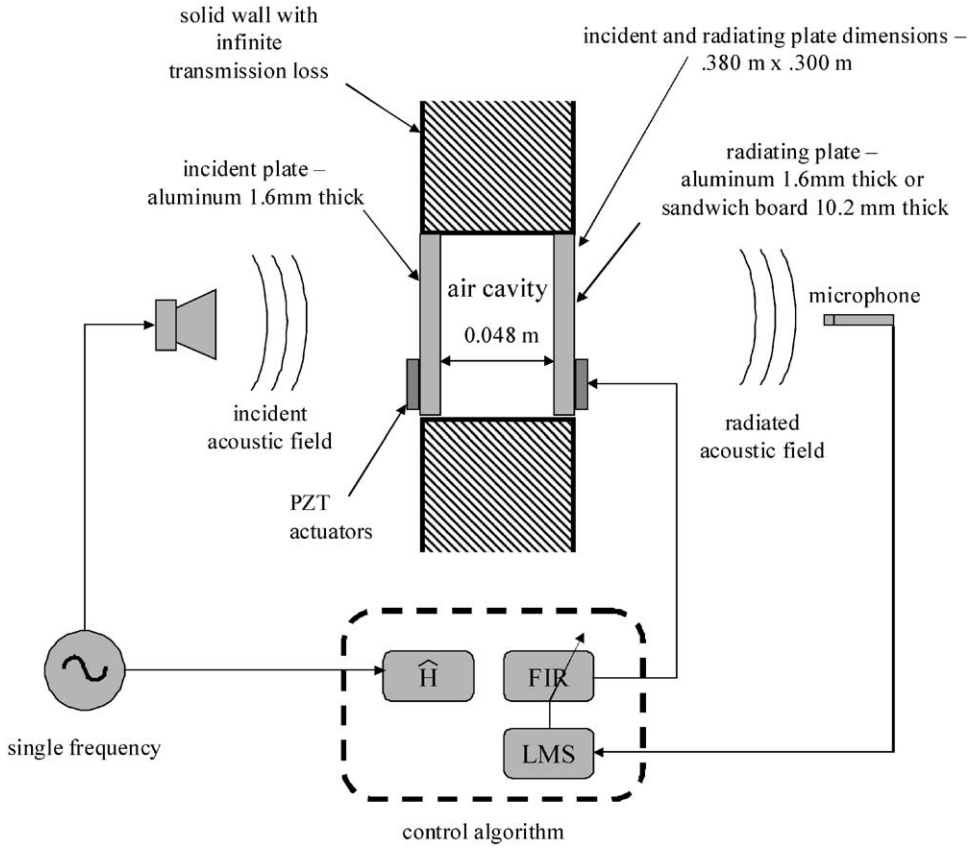

Fig. 1. Schematic of active structural acoustic control of double panel systems.

be excited by an oblique incident acoustic plane wave. The defined cost function for the control analysis is radiated acoustic power, which is determined by integrating the acoustic pressure in the far field over a hemisphere surrounding the radiating plate. Control signals are output to four piezoelectric actuators that are placed so that each actuator is evenly spaced at the corner of a rectangle on the plate. The actuator placement was chosen so each could couple into every plate mode up to the (4,4) mode. Control inputs are determined by linear quadratic optimal control theory (LQOCT) [2]. Specifies of the structural, acoustic, and controller analytical models are now discussed.

2.2. Structural models

In this section, double panel system structural models are presented. The general assumptions are (1) the system has a steady state sinusoidal response, and (2) the spatial response of all of the governing differential equations can be represented by an infinite series of eigenfunctions. Therefore, the response can be written as a homogeneous solution of the modal amplitudes and eigenvectors. An additional assumption is the plates have simply supported boundary conditions for derivation of the eigenvectors and eigenvalues, and then the model will be modified for clamped boundary conditions. The modal amplitudes are then determined by the application of a specific forcing function.

2.2.1. Double panel system

The following derivations are based on those originally performed by Vaicaitis [3] and the reader is referred to this reference for specifics. The double panel system considered in this investigation consists of two simply supported single plates separated by an air cavity as seen in Fig. 1. This configuration approximates the fuselage (incident plate) and internal trim (radiating plate) of modern aircraft. The air cavity between the two plates can be analytically described as a uniformly distributed linear air spring (K_s) which acts on the relative displacement of the two plates. This assumption is valid well below the first transverse resonance of the air cavity [3], which is 3572 Hz. The governing equations of motion describing the out-of-plane displacement (w) for the double panel system can be written as

$$\begin{aligned} m_i\ddot{w}_i + C_i\dot{w}_i + D_i\nabla^4 w_i + K_s(w_i - w_r) + \left(\frac{1}{3}\right)m_s\ddot{w}_i + \left(\frac{1}{6}\right)m_s\ddot{w}_r = 0,\\ m_r\ddot{w}_r + C_r\dot{w}_r + D_r\nabla^4 w_r + K_s(w_r - w_i) + \left(\frac{1}{3}\right)m_s\ddot{w}_r + \left(\frac{1}{6}\right)m_s\ddot{w}_i = 0, \end{aligned} \tag{1}$$

where

$$\nabla^4 = \frac{\partial^4}{\partial x^4} + 2\frac{\partial^4}{\partial x^2\partial y^2} + \frac{\partial^4}{\partial y^4}, \quad \begin{aligned} m_i &= \rho_i h_i, \quad D_i = \frac{E_i h_i^3}{12(1-\upsilon_i^2)},\\ m_r &= \rho_r h_r,\\ m_s &= \rho_s h_s, \quad D_r = \frac{E_r h_r^3}{12(1-\upsilon_r^2)}, \end{aligned} \tag{2}$$

where w_i and w_r are the flexural displacements of the incident and radiating plates, respectively. Subscripts i, r, and s denote the incident plate, the radiating plate and the air space, respectively. The air spring (K_s) is modelled as a linear elastic spring with no damping:

$$K_s = \frac{E_s}{h_s} = \frac{\rho_s c^2}{h_s}, \tag{3}$$

which acts on the relative displacement of the two plates. It was assumed that the inertial force varied linearly across the air space and therefore the air inertia terms ($m_s/3$ and $m_s/6$) were apportioned to the individual plates. For further explanation of this concept, the reader is referred to Vaicaitis [3].

The flexural response of the individual plates can be written as the summation of the product of the modal amplitudes and the eigenvectors, which satisfy the simply supported boundary conditions. Substituting the assumed solution into the equations of motion and utilizing the orthogonality principle yields a set of coupled differential equations [3]. After algebraic manipulation, the frequency response functions (Θ) can be written as a function of the excitation frequency (ω) and the natural frequencies (ω_{mn}) for the incident plate as

$$\begin{aligned} \Theta^i_{mn} &= \frac{X^i_{mn}}{1 - \left(E_s/h_s + \omega^2 b_s\right)^2 \left(X^i_{mn}/m_i\right)\left(X^r_{mn}/m_r\right)}, \\ \Theta^r_{mn} &= \Theta^i_{mn}\left(\frac{E_s}{h_s} + \omega^2 b_s\right)^2 \left(\frac{X^r_{mn}}{m_r}\right) \end{aligned} \tag{4}$$

and for a forcing function acting on the radiating plate

$$\begin{aligned} \Theta^r_{mn} &= \frac{X^r_{mn}}{1 - \left(E_s/h_s + \omega^2 b_s\right)^2 \left(X^i_{mn}/m_i\right)\left(X^r_{mn}/m_r\right)}, \\ \Theta^i_{mn} &= \Theta^r_{mn}\left(\frac{E_s}{h_s} + \omega^2 b_s\right)^2 \left(\frac{X^i_{mn}}{m_i}\right), \end{aligned} \tag{5}$$

where

$$\begin{aligned} X^i_{mn} &= \left[(\omega^i_{mn})^2 - \left(\frac{a_i}{m_i}\right)\omega^2 + 2\mathrm{j}\omega^i_{mn}\omega\eta^i_{mn} + \frac{E_s}{h_s m_i}\right]^{-1}, \\ X^r_{mn} &= \left[(\omega^r_{mn})^2 - \left(\frac{a_r}{m_r}\right)\omega^2 + 2\mathrm{j}\omega^r_{mn}\omega\eta^r_{mn} + \frac{E_s}{h_s m_r}\right]^{-1}, \end{aligned} \tag{6}$$

$$a_i = m_i + \frac{m_s}{3}, \quad a_r = m_r + \frac{m_s}{3}, \quad b_s = \frac{m_s}{6}. \tag{7}$$

In the above equations, the uncoupled natural frequencies of the incident and radiating plates, respectively, are defined as

$$\omega^i_{mn} = \left(\frac{D_i}{m_i}\right)^2 (\alpha_m^2 + \alpha_n^2), \quad \omega^r_{mn} = \left(\frac{D_r}{m_r}\right)^2 (\alpha_m^2 + \alpha_n^2). \tag{8}$$

The natural frequencies of the double panel system can be determined by setting the damping to zero and maximizing the frequency response functions in Eqs. (4) and (5):

$$\omega_{mn} = \sqrt{\frac{B_{mn} \pm \sqrt{B_{mn}^2 - 4AC_{mn}}}{2A}}, \tag{9}$$

where

$$\begin{aligned} A &= a_i a_r - b_s^2, \\ B_{mn} &= \left(m_i \omega_{mn}^{i^2} + \frac{E_s}{h_s}\right) a_r + \left(m_r \omega_{mn}^{r^2} + \frac{E_s}{h_s}\right) a_i + 2b_s \frac{E_s}{h_s}, \\ C_{mn} &= \left(m_i \omega_{mn}^{i^2} + \frac{E_s}{h_s}\right)\left(m_r \omega_{mn}^{r^2} + \frac{E_s}{h_s}\right) - \left(\frac{E_s}{h_s}\right)^2. \end{aligned} \tag{10}$$

These equations give two real eigenvalues for each set of modal indices. For each modal index, the eigenvalue with the lower value corresponds to the in-phase flexural response and eigenvalue with the higher value corresponds to the out-of-phase dilatation response of the double panel system. Physically, the in-phase flexural response is when the displacement of the two plates comprising the double panel system is in-phase, i.e. both plates travel in the positive z direction at the same instant. The out-of-phase dilatational response [3] is when the displacement of the two plates is out-of-phase, i.e. one plate travels in the positive z direction and the other travels in the negative z direction. Physically, there is little or no relative displacement between the individual plates which means that the spring rate of the acoustical cavity has little effect for the in-phase flexural motion. For the out-of-phase dilatational motion, the relative displacement between the plates is significant and the increased stiffness (due to the spring rate of the acoustical cavity) of the system results in an increased natural frequency. This will be discussed further in the results section.

2.2.2. *Clamped boundary conditions*

The above analyses were performed for simply supported boundary conditions. To be able to experimentally verify the models, simply supported boundary conditions are difficult if not impossible to implement for determining transmission loss. The accepted method for experimentally investigating transmission loss includes plates mounted in a frame in an extended wall that approximates clamped boundary conditions and allows no acoustical transmission path. This method also reduces other factors such as structure-borne flanking transmission paths, which can taint the results of the transmission loss experiments. Due to the above conditions, the theoretical models must be modified to approximate clamped boundary conditions.

Although simply supported mode shapes have been shown to be a reasonable approximation of clamped mode shapes [3,4] the associated simply supported natural frequencies are incorrect due to the lack of stiffness inherent to the simply supported boundary conditions compared to the clamped boundary conditions. As an approximation, the stiffness of the simply supported plate can be increased by $\sqrt{2}$ for each boundary [3] to approximate the clamped boundary conditions and therefore the natural frequencies will more accurately represent clamped boundary conditions. This modification can be inferred from a comparison of a simply supported beam

(or plate) natural frequencies compared to a clamped beam (or plate) [4]. This has been shown to have little effect on the validity of the theoretical model [3] since the difference in modal radiation efficiencies of clamped and simply supported plates has been shown to be less than 3 dB [5].

2.3. Acoustic models

2.3.1. Incident pressure field

The incident pressure field is assumed to be an oblique incident plane wave which impinges on the incident side of the single plate or the incident plate of the double panel system. The mathematical expression for the plane wave can be written as [6]

$$p_i(x,y,t) = P_i \exp[\mathrm{j}(\omega t - kx\sin\theta_i\cos\phi_i - ky\sin\theta_i\sin\phi_i - kz\cos\theta_i)]. \tag{11}$$

Further discussion of the incident pressure field as a forcing function is presented in the next section. The incident intensity is the amount of intensity that is normal to the plate,

$$I_i = \frac{P_i^2\cos\theta_i}{2\rho c}. \tag{12}$$

The incident acoustic power is the incident intensity times the area of the plate,

$$\Pi_i = \frac{P_i^2\cos\theta_i l_x l_y}{2\rho c}. \tag{13}$$

2.3.2. Radiated pressure field

The radiated pressure field emits from the radiating side of a single plate or the radiating plate of a double panel system. The equation for the radiated pressure from a plate is derived from the model of the radiated pressure from an elementary volume source mounted in an infinite rigid baffle [6]. From an acoustical viewpoint, the motion of the plate can be seen as a multitude of these elementary volume sources. Therefore, the total radiation from a plate can be found by integrating the radiated pressure from an elementary volume source over the domain of the plate. The result is the well-known Rayleigh integral for a plate [7]. For these calculations, the numerical values for the plate were previously given in Section 2.1, and the wavelength is equal to (c/frequency).

Utilizing the far field approximation, which is valid if the radius at which the pressure is being evaluated, is large compared to the maximum dimension of the structure, a closed form solution for the Rayleigh integral is [6]

$$p_r(r,\theta,\phi) = -\frac{\omega^2\rho_o l_x l_y}{2\pi r}\exp\left\{\mathrm{j}\omega\left[t - \frac{r}{c} - \frac{\sin\theta}{2c}(l_x\cos\phi + l_y\sin\phi\right]\right\}\sum_{m=1}^{\infty}\sum_{n=1}^{\infty} W_{mn}Y_mY_n, \tag{14}$$

where

$$Y_m = \begin{cases} -\dfrac{\mathrm{j}}{2}\mathrm{sgn}(\sin\theta_r\cos\phi_r), & ((m\pi)^2 = [\sin\theta_r\cos\phi_r(\omega l_x/c)]^2), \\ \dfrac{m\pi\{1-(-1)^m\exp[-\mathrm{j}\sin\theta_r\cos\phi_r(\omega l_x/c)]\}}{(m\pi)^2 - [\sin\theta_r\cos\phi_r(\omega l_x/c)]^2}, & ((m\pi)^2 \neq [\sin\theta_r\cos\phi_r(\omega l_x/c)]^2), \end{cases}$$

$$Y_n =, \begin{cases} -\frac{\mathrm{j}}{2}\mathrm{sgn}(\sin\theta_r \cos\phi_r), & ((n\pi)^2 = [\sin\theta_r \cos\phi_r(\omega l_y/c)]^2), \\ \dfrac{n\pi\{1-(-1)^n \exp[-\mathrm{j}\sin\theta_r \cos\phi_r(\omega l_y/c)]\}}{(n\pi)^2 - [\sin\theta_r \cos\phi_r(\omega l_y/c)]^2}, & ((n\pi)^2 \neq [\sin\theta_r \cos\phi_r(\omega l_y/c)]^2). \end{cases} \tag{15}$$

As a result of the far field assumption, the pressure wave can be locally approximated by a plane wave. Therefore the far field intensity at a point can be written as

$$I_r = \frac{|p_r(r,\theta,\phi)|^2}{2\rho c}. \tag{16}$$

The total radiated power is defined as the integral of the far field intensity over a hemisphere enclosing and centered on the baffled plate which can be written as

$$\Pi_r = \int_{\phi=0}^{2\pi}\int_{\theta=0}^{\pi/2} I_r r^2 \sin\theta \,\mathrm{d}\theta \,\mathrm{d}\phi. \tag{17}$$

2.3.3. Transmission loss

The plate transmission loss is defined as [8]

$$TL(\mathrm{dB}) = 10\log_{10}\left(\frac{1}{\tau}\right) = 10\log_{10}\left(\frac{\Pi_i}{\Pi_r}\right). \tag{18}$$

For engineering design, it is useful to have a single acoustic performance index that can be compared. Therefore, the transmission loss will be averaged over a frequency range. This index is more applicable than frequency dependent power reduction since the disturbance is tonal in nature and the frequency varies. The frequency averaged transmission loss is defined as

$$TL_{avg}(\mathrm{dB}) = 10\log_{10}\left(\frac{\Pi_{i,avg}}{\Pi_{r,avg}}\right), \tag{19}$$

where the frequency averaged acoustic power is defined as

$$\Pi_{avg} = \frac{1}{N}\sum_{n=1}^{N}\Pi_n. \tag{20}$$

Note that this assumes the transmission loss data is discrete over the frequency range. The frequency averaged acoustic power is a linear average of the auto-spectrum which denotes the average power over a frequency range. Note that the analytical results are presented in terms of frequency averaged transmission loss.

2.4. Plate forcing functions

2.4.1. Incident pressure field

When the incident pressure field impinges on the plate, there are two traveling waves incident upon the double panel system incident plate, the incident pressure and the reflected pressure. Conversely, only one traveling wave, the radiated pressure, emits from the radiating plate of the double panel system. In previous analyses, it was found that the incident and reflected pressure

wave magnitudes can be assumed equal since the impedance of the plate approximates a rigid boundary for air loading [8]. Therefore, the pressure exciting the plate is assumed to be the *blocked* pressure, which is twice the magnitude of the incident wave. The inclusion of the radiated pressure into the solution of the non-homogeneous solution of the plate motion produces a very complicated equation known as the *fluid loaded* plate equation. However when the fluid is air, it was found that the transmitted pressure was negligible compared to the blocked pressure [6]. Without the radiated pressure term, the equation of motion of the plate can readily be solved for the *in-vacuo* (which is sometimes called *light fluid loaded) case*.

As stated earlier, the forcing function can be decomposed into an infinite series of eigenfunctions. The blocked pressure can be represented as

$$p_b = 2p_i(x,y,t) = \sum_{m=1}^{\infty}\sum_{n=1}^{\infty} p_{mn}^d \sin(\alpha_m x)\sin(\alpha_n y), \tag{21}$$

where p_i was defined in Eq. (11) and

$$p_{mn}^d = \frac{8P_i}{l_x l_y}\int_{x=0}^{l_x}\int_{y=0}^{l_y} \exp[\mathrm{j}(kx\sin\theta_i\cos\phi_i - ky\sin\theta_i\sin\phi_i)]\sin(\alpha_m x)\sin(\alpha_n y)\,\mathrm{d}y\,\mathrm{d}x. \tag{22}$$

This integration has a closed form solution:

$$p_{mn}^d = 8P_i Y_m Y_n, \tag{23}$$

where Y_m and Y_n are defined as

$$Y_m = \begin{cases} -\dfrac{\mathrm{j}}{2}\mathrm{sgn}(\sin\theta_i\cos\phi_i), & ((m\pi)^2 = [\sin\theta_i\cos\phi_i(\omega l_x/c)]^2), \\ \dfrac{m\pi\{1-(-1)^m\exp[-\mathrm{j}\sin\theta_i\cos\phi_i(\omega l_x/c)]\}}{(m\pi)^2 - [\sin\theta_i\cos\phi_i(\omega l_x/c)]^2}, & ((m\pi)^2 \neq [\sin\theta_i\cos\phi_i(\omega l_x/c)]^2), \end{cases}$$

$$Y_n = \begin{cases} -\dfrac{\mathrm{j}}{2}\mathrm{sgn}(\sin\theta_i\cos\phi_i), & ((n\pi)^2 = [\sin\theta_i\cos\phi_i(\omega l_y/c)]^2), \\ \dfrac{n\pi\{1-(-1)^n\exp[-\mathrm{j}\sin\theta_i\cos\phi_i(\omega l_y/c)]\}}{(n\pi)^2 - [\sin\theta_i\cos\phi_i(\omega l_y/c)]^2}, & ((n\pi)^2 \neq [\sin\theta_i\cos\phi_i(\omega l_y/c)]^2). \end{cases} \tag{24}$$

Note that the above expression is the same as defined in Eq. (15) except the angles are radiating co-ordinates compared to Eq. (24) which uses incident co-ordinates. The modal amplitudes can now be written for a double panel system by multiplying the modally decomposed disturbance (Eq. (23)) by the frequency response function for a forcing function acting on the incident plate (Eq. (4)):

$$W_{mn}^{d,i} = p_{mn}^d \Theta_{mn}^i, \quad W_{mn}^{d,r} = p_{mn}^d \Theta_{mn}^r. \tag{25}$$

2.4.2. Piezoelectric actuator

Piezoelectric plate actuators generally consist of a lead zirconate titanate (PZT) actuator co-located pair (on each side of the plate) wired out of phase to produce pure bending in the structure. Their forcing function can be modelled as line moments applied at the PZT element boundary. Following the solution for the incident pressure field, the PZT forcing function can be

decomposed into an infinite series of eigenfunctions. Using mode orthogonality, the modally decomposed forcing function can be written [9]

$$\bar{P}^c_{mn} = 4C_o\varepsilon_{pe}\left(-\frac{\alpha_x^2+\alpha_y^2}{\alpha_x\alpha_y}\right)[\cos(\alpha_x x_1)-\cos(\alpha_x x_2)][\cos(\alpha_y y_1)-\cos(\alpha_y y_2)], \tag{26}$$

where $\varepsilon_{pe} = (d_{3l}V/t)$ and C_o is a constant. This term is a constant that is a function of the plate and piezo actuator properties and geometry.

The modal amplitudes can now be written for a PZT actuator by multiplying the modally decomposed disturbance (Eq. (26)) by the double panel system frequency response function for a forcing function:

$$W^{c,r}_{mn} = p^c_{mn}\Theta^r_{mn}, \quad W^{c,i}_{mn} = p^c_{mn}\Theta^i_{mn}, \tag{27}$$

where Θ^i_{mn} and Θ^r_{mn} were defined in Eqs. (4) and (5) for a piezoelectric actuator mounted on the incident and radiating plates, respectively. The PZT properties are presented in Table 1.

2.4.3. Total structural response

The total structural response of the system can be determined by the superposition of the system response to the disturbance (the incident pressure field in this paper) and the control field defined as the sum of each piezoelectric actuator response. The total modal response of the system can be written:

$$W^{t,i}_{mn} = W^{d,i}_{mn} + \sum_{j=1}^{C} W^{c_j,i}_{mn}, \quad W^{t,r}_{mn} = W^{d,r}_{mn} + \sum_{j=1}^{C} W^{c_j,r}_{mn}, \tag{28}$$

where C is the total number of piezoelectric actuators.

2.4.4. Cost function

The stated objective is the reduction of the transmission loss of a double panel system. This is accomplished by reducing the radiated sound power emitted by the radiating plate of a double panel system, which can be written for a baffled plate as

$$\Pi_r = \frac{1}{\rho c}\int_0^{2\pi}\int_0^{\pi/2} |p_r(r,\theta,\phi)|^2 r^2 \sin\theta \, d\theta \, d\phi, \tag{29}$$

Table 1
PZT properties

Material	Lead zirconate titanate
Density (kg/m^3)	7600
Strain coefficient (m/V)	166E−12
Elastic modulus (N/m^2)	63E+9

where p_r is the far field pressure. Writing Eq. (29) in terms of the total modal response of the radiating plate and rearranging:

$$\Pi_r = \sum_{m=1}^{\infty}\sum_{n=1}^{\infty}\sum_{k=1}^{\infty}\sum_{l=1}^{\infty} \Delta_{mnkl} W_{mn}^{t,r} W_{kl}^{t,r*}, \tag{30}$$

where [10]

$$\Delta_{mnkl} = \frac{1}{\rho c}\int_0^{2\pi}\int_0^{\pi/2} AA^* Y_m Y_n Y_k^* Y_l^* r^2 \sin\theta \, \mathrm{d}\theta \, \mathrm{d}\phi \tag{31}$$

and where Y_m was previously defined in Eq. (15) and

$$A = -\frac{\omega^2 \rho_o l_x l_y}{2\pi r} \exp\left\{ \mathrm{j}\omega \left[t - \frac{r}{c} - \frac{\sin\theta}{2c}(l_x \cos\phi + l_y \sin\phi \right] \right\}. \tag{32}$$

2.4.5. Linear quadratic optimal control

For the analytical results, LQOCT is used to determine the optimal control inputs for the application of ASAC to double panel systems. The reduction of the transmission loss of a double panel system is accomplished in practice by reducing the radiated sound power from the radiating panel of a double panel system, which was previously written in Eq. (30). Using superposition, the total modal response of the radiating panel can be written as a function of the applied piezoelectric force, which is a function of applied voltage (V).

$$W_{mn}^{t,r} = W_{mn}^{d,r} + \sum_{i=1}^{C} \Psi_{mn}^{c_i,r} V_i, \tag{33}$$

where $W_{mn}^{c_i,r} = \Psi_{mn}^{c_i,r} V_i$ and Ψ has dimensions m/V. It is evident from the substitution of Eq. (33) into Eq. (30) that the radiated sound power is a quadratic function of the applied piezoelectric voltage. Taking the derivative of radiated power with respect to the piezoelectric voltage (the control signal to each actuator) and setting the result equal to zero will give the equation for the optimal applied piezoelectric voltage:

$$\begin{Bmatrix} V_1 \\ \vdots \\ V_C \end{Bmatrix} = \begin{bmatrix} \beta \Psi_{mn}^{c_1,r} \Psi_{mn}^{c_1,r*} & \cdots & \beta \Psi_{mn}^{c_1,r} \Psi_{mn}^{c_C,r*} \\ \vdots & \ddots & \vdots \\ \beta \Psi_{mn}^{c_C,r} \Psi_{mn}^{c_1,r*} & \cdots & \beta \Psi_{mn}^{c_C,r} \Psi_{mn}^{c_C,r*} \end{bmatrix}^{-1} \begin{Bmatrix} -\beta W_{mn}^{d,r} \Psi_{mn}^{c_1,r*} \\ \vdots \\ -\beta W_{mn}^{d,r} \Psi_{mn}^{c_C,r*} \end{Bmatrix}, \tag{34}$$

where

$$\beta = \sum_{m=1}^{\infty}\sum_{n=1}^{\infty}\sum_{k=1}^{\infty}\sum_{l=1}^{\infty} \Delta_{mnkl}. \tag{35}$$

3. Results

Analytical results calculated from the double panel system, acoustic, and controller models developed in the previous section are presented. First, the analytical double panel system model is

validated through a comparison of the theoretical and experimental uncontrolled transmission loss. The analytical model is then applied to the active control of double panel systems and a parametric analysis including the variation of the location of control actuators, the radiating plate stiffness, and the air cavity mass and stiffness.

3.1. Model validation

The analytical double panel system model is validated through a comparison of the theoretical and experimental uncontrolled transmission loss for an aluminum and sandwich board radiating plate double panel system. The system is described as follows: a normal acoustic plane wave excites the incident plate of a double panel system. The induced incident plate motion excites the acoustic cavity thereby inducing motion in the radiating plate. The radiating plate then emits acoustic power into an acoustic free field. For experimental implementation, the incident acoustic field was provided by a speaker positioned adjacent to the incident plate of the double panel system at a distance of 0.3 m to provide an approximation of a plane wave. A broadband signal of 0–800 Hz was input to the speaker providing excitation of the double panel system. Incident pressure measurements were taken by a single microphone positioned near the center of the incident plate. Radiated pressure measurements were taken by a microphone positioned at several points on a hemisphere in an anechoic room. The hemisphere was divided into equal areas and one microphone was placed at the center of each area. From the microphone measurements and associated area, an approximation of radiated acoustic power can then be calculated. All pressure measurements were processed by a B&K model 2032 dual channel signal analyzer where the auto-correlation and cross-correlation of the disturbance signal and the pressure measurements were computed. This information was downloaded to a PC compatible computer and analyzed using a MATLAB code which yielded the transmission loss data as per calculations detailed previously. The signal levels at the incident plate were approximately 110 dB to achieve approximate signal levels of 70 dB (off-resonance) in the anechoic room. Comparison to aircraft levels depends on the specific aircraft configuration, but this level is within an order of magnitude for a trimmed aircraft.

A comparison of the theoretical and experimental uncontrolled transmission loss of the aluminum radiating plate double panel system is shown in Fig. 2. Note that the theoretical curve does not exist below 50 Hz since this was the approximate frequency where the flanking paths of the test facility dominate the experimental results. The results indicate that the transmission loss minima correspond to the natural frequencies of the system with the most prominent occurring at the in-phase and out-of-phase (1,1) ($\sim$120–170 Hz), (3,1) ($\sim$350–360 Hz), and (1,3) ($\sim$490–500 Hz) modes. This agrees with the theoretical model for an normal plane wave which indicates that a uniform excitation field can only excite the symmetric modes, i.e. modes that have an odd–odd index. However, the experimental results show minima at other natural frequencies of the double panel system, namely the (1,2) ($\sim$260–280 Hz) and (4,1) ($\sim$520–560 Hz) modes. The excitation of these modes could be attributed to a number of things including an imperfect normal acoustic plane wave, unevenly damped plate, and/or the structural flanking path. As stated earlier, the intent is to provide a model to investigate the *trends* involved with active control of double panel systems. As can be seen in Fig. 2, there is general agreement in the trend of the theory with experiment.

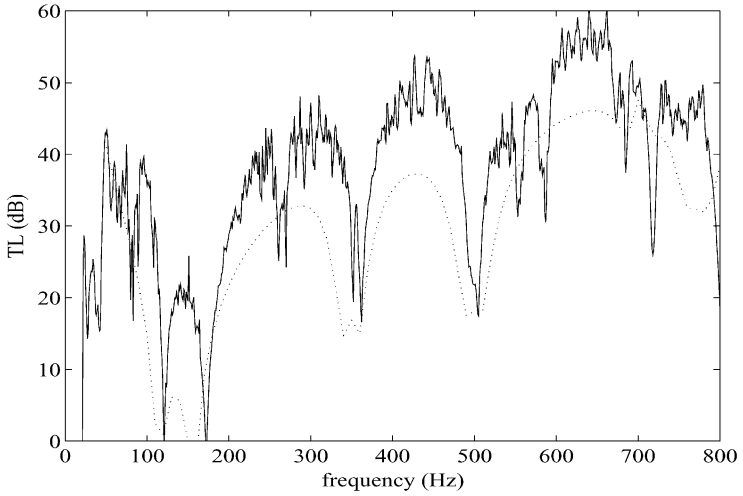

Fig. 2. Uncontrolled aluminum radiating plate double panel system TL: · · · ·, theoretical; ——, experimental.

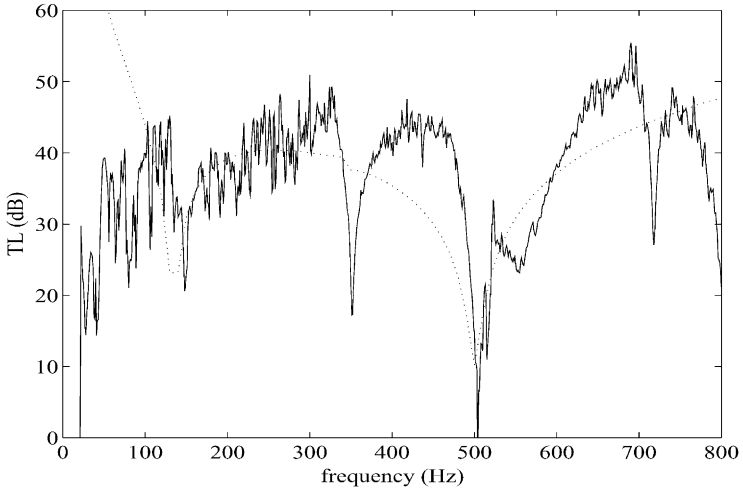

Fig. 3. Uncontrolled sandwich board radiating plate double panel system TL: · · · ·, theoretical; ——, experimental.

A comparison of the theoretical and experimental uncontrolled transmission loss of the sandwich board radiating plate double panel system is shown in Fig. 3. In this plot, the prominent transmission loss minima occur at the in-phase (1,1) mode ($\sim$135 Hz), the in-phase (3,1) mode ($\sim$350 Hz) and the out-of-phase (1,1) mode ($\sim$500 Hz). Notice there are less minima compared to the aluminum radiating plate double panel system (Fig. 2) due to the lower modal density, as a result of the increased stiffness of the sandwich board radiating plate. It should be noted that the values of transmission loss are significantly higher (as compared to Fig. 2) in the low frequency range of 100–200 Hz due to the absence of an efficient acoustic radiating mode resonance. These results agree with Carneal and Fuller [1] who found that a stiff radiating plate exhibited increased uncontrolled transmission loss over a more flexible radiating plate. The above results also agree

with fundamental transmission loss theory. According to Fahy [8], plate response is stiffness controlled at low frequencies. A plate with increased stiffness leads to lower response, which leads to higher transmission loss.

In summary, the theoretical and experimental results show good agreement in the double panel system trends in uncontrolled transmission loss. Further improvements in modelling of the incident acoustic field and/or the double panel system boundary conditions could possibly minimize the detailed discrepancies seen in transmission loss curves.

3.2. Active control of double panel systems

This section theoretically investigates the active control of double panel systems using the previously defined models. The results are presented in several subsections that provide insight to the active control of double panel systems by perturbing the basic double panel system parameters. Specifically, the influence of the following double panel system parameters on control performance is studied: the radiating plate stiffness (aluminum or sandwich board), PZT actuator location (incident or radiating plate), and air cavity parameters (mass and stiffness).

In this and the following sections, the compound adjectives associated with a full system description can become excessive. For instance, for the PZT location parameter, the full description of the double panel system would be a *sandwich board radiating plate double panel system with incident plate PZT locations.* In this paper, this full description will be stated only once for brevity. Once the full description has been stated, an abbreviated description using the word *case* will be used. For example, the above description will be shortened to the *incident PZT case*.

3.2.1. Effect of radiating plate stiffness on control performance

The first parameter to be studied is the radiating plate stiffness where an aluminum radiating plate is used for a relatively flexible case and a sandwich board is used for a relatively stiff case. The effect of radiating plate stiffness on the increase in frequency averaged transmission loss (TL_{avg}, as defined in Eq. (19)) with control is presented in Table 2 (along with the variation of the test system parameters of incident plane wave and PZT location). The increase in TL_{avg} is presented for two distinct averages, one from 50 to 800 Hz and 300 to 800 Hz. Two distinct averaging ranges are presented since some of the results obtained are also dependent upon the variation of the frequency range.

Table 2
Effect of radiating plate stiffness on increase in frequency averaged transmission loss with control

PZT location	Incident wave	Radiating plate			
		Aluminum	Sandwich board	Aluminum	Sandwich board
		Increase in TL_{avg} (dB) 50–800 Hz		Increase in TL_{avg} (dB) 300–800 Hz	
Incident	Normal	30.0	49.1	11.4	22.6
	Oblique	30.3	48.8	11.0	22.9
Radiating	Normal	23.8	53.6	12.3	39.9
	Oblique	24.2	53.4	10.8	38.3

As can be seen in Table 2, better control is achieved for a double panel system with a sandwich board radiating plate over an aluminum radiating plate by approximately 11–30 dB depending on the other system parameters. The explanation for this behavior is due to the modal density of the double panel system. This behavior will now studied in more detail.

Fig. 4 shows the uncontrolled and controlled transmission loss versus frequency for a double panel system excited by an oblique incident wave with the PZTs actuators located on an aluminum radiating plate. As compared to results for the same test configuration except with a sandwich board radiating plate (Fig. 5), the aluminum case exhibits several more TL minima compared to the sandwich board case, which indicates the aluminum case has a higher modal

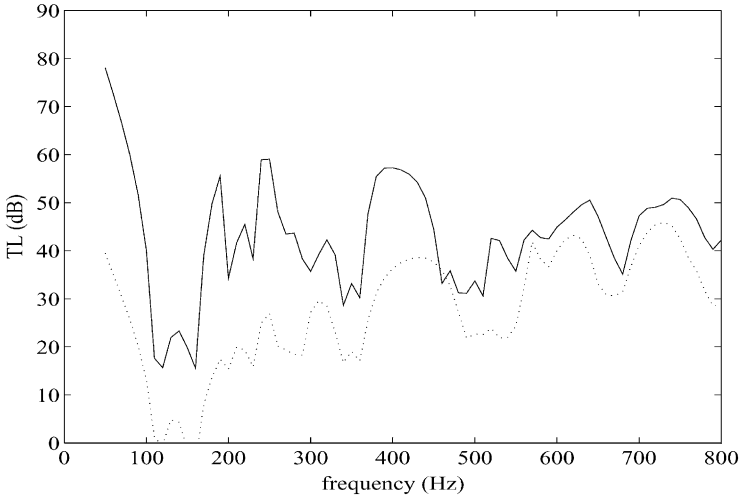

Fig. 4. Uncontrolled and controlled transmission loss for double panel system with aluminum radiating plate (other parameters: oblique incident wave; radiating plate PZT location): · · · ·, uncontrolled; ——, controlled.

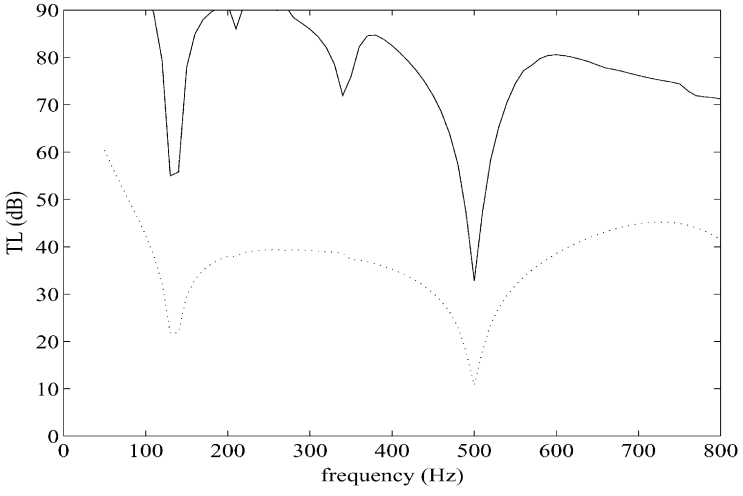

Fig. 5. Uncontrolled and controlled transmission loss for double panel system with sandwich board radiating plate (other parameters: oblique incident wave; radiating plate PZT location): · · · ·, uncontrolled; ——, controlled.

density. Since the amount of achievable control attenuation is directly related to the number of control channels with respect to the number of system dominant modes (and the controllability of those modes), a double panel system with a higher modal density at a certain frequency will attain less control reduction in sound than one with a low modal density for a given number of control actuators [11]. Also, a stiffer radiating plate leads to lower response and therefore lower sound radiation over the entire frequency range. However, the coupling of the incident and radiating plate through the contained air is much less for the sandwich board case. As seen in Fig. 6, the modal response of a double panel system with a sandwich board radiating plate excited at the out-of-phase fundamental resonance ($f = 500$ Hz) shows that control of the radiating plate has little effect on the incident plate. This type of behavior is typical for the sandwich board case and is independent of excitation frequency. This is a result of the low modal density of the radiating plate. Control is achieved by modal reduction which reduces the overall response of the radiating plate [11]. Since the incident and radiating plate are not well coupled, the influence of the control actuators on the incident plate is minimal.

Control effort, defined as the sum of the absolute value of the control voltages squared calculated in Eq. (34), for a double panel system excited by an oblique incident wave and with PZT actuators mounted on the radiating plate is shown in Fig. 7. As can be seen in this figure, a double panel system with an aluminum radiating plate requires more control effort (power) than one with a sandwich board radiating plate. At first this seems to be an erroneous result since the sandwich board radiating plate is much stiffer than the aluminum radiating plate. However, the sandwich board radiating plate is also thicker than the aluminum radiating plate. The end result is that the sandwich board radiating plate PZT forcing function (p^c_{mn} in Eq. (26) with a unit applied PZT voltage (V)) is an order of magnitude greater than the one for an aluminum radiating plate. This is due to a better impedance matching of the PZT actuator with the stiff radiating plate.

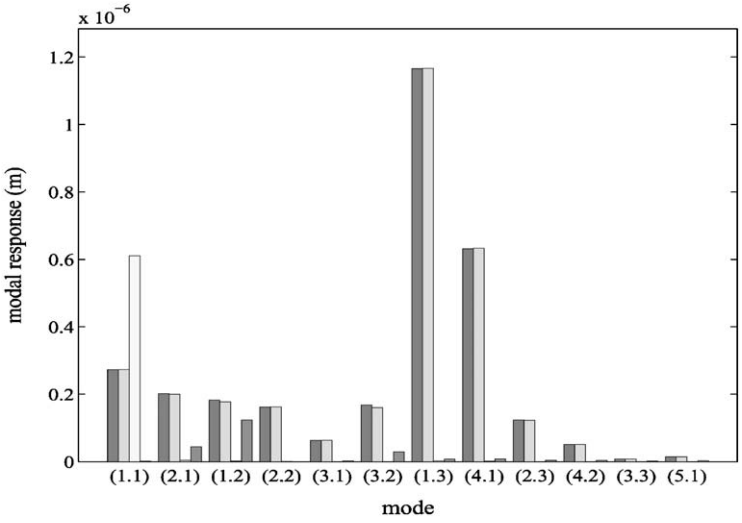

Fig. 6. Uncontrolled and controlled double panel system modal amplitudes at 500 Hz with sandwich board radiating plate (other parameters: oblique incident wave; radiating plate PZT location): ■, uncontrolled incident plate; □, controlled incident plate; □, uncontrolled radiating plate; □, controlled radiating plate.

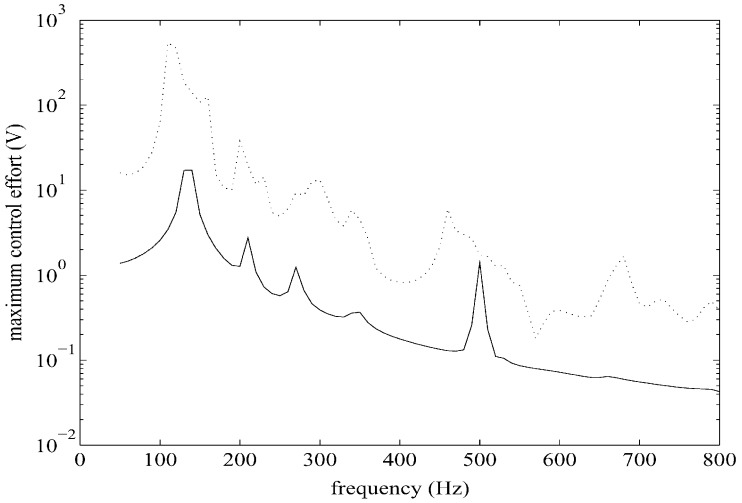

Fig. 7. Maximum control effort for a double panel system with an aluminum and sandwich board radiating plate (other parameters: oblique incident wave; PZTs located on radiating plate): · · · ·, aluminum; ——, sandwich board.

Table 3
Effect of PZT location on increase in frequency averaged transmission loss with control

Radiating plate	Incident wave	PZT location			
		Incident	Radiating	Incident	Radiating
		Increase in TL_{avg} (dB) 50–800 Hz		Increase in TL_{avg} (dB) 300–800 Hz	
Aluminum	Normal	30.0	23.8	11.4	12.3
	Oblique	30.3	24.2	11.0	10.8
Sandwich board	Normal	49.1	53.6	22.6	39.9
	Oblique	48.8	53.4	22.9	38.3

3.2.2. *Effect of PZT location on control performance*

In this section, the effect of the location of the control actuators on double panel system control performance is presented. The control actuators (PZT piezoelectric actuators) can be positioned either on the incident or radiating plate of the double panel system and will be referred to as the *incident PZT case* and the *radiating PZT case.* As can be seen in Table 3, the effect of PZT location on frequency averaged transmission loss (TL_{avg}) depends on the choice of radiating plate stiffness and the range over which the transmission loss was averaged. For an aluminum radiating plate with control performance averaged from 50 to 800 Hz, the incident PZT case attained approximately 6 dB more TL_{avg} than the radiating PZT case. Looking at the performance numbers for the 300–800 Hz averaged transmission loss, the incident PZT case indicates no advantage for the aluminum radiating plate double panel system. However, for the sandwich board radiating plate double panel system, the radiating PZT case performs better than the incident PZT case regardless of the transmission loss averaging range. This behavior will now be discussed in more detail.

The uncontrolled and controlled transmission loss for a double panel system with a sandwich board radiating plate and excited by an oblique plane wave is shown in Fig. 8. Control of the system with PZTs mounted on the radiating plate is more effective by approximately 20 dB at frequencies above 300 Hz. This behavior can be explained by how well the control actuators can influence the structural-acoustic coupling of the radiating plate and the radiating acoustic field. As stated in the previous section, the motion of the incident plate is not significantly coupled into the motion of the sandwich board radiating plate and therefore is not coupled significantly into the radiated acoustic field. The PZT actuators on the incident plate will not be able to significantly modify structural-acoustic coupling of the radiated plate. However, actuators mounted on the radiating plate can directly modify the structural-acoustic coupling and therefore better control is achieved.

The results for an aluminum radiating plate double panel system are not as definite. Fig. 9 shows the uncontrolled and controlled transmission loss for an aluminum radiating plate double panel system excited by a normal incident plane wave. As can be seen, the effect of the PZT location on control performance varies with frequency. From an investigation of the double panel system equations, it is seen that a double panel system consisting of two plates of similar properties will exhibit behavior where one plate will dominate the double panel system response over some frequency ranges, while the other plate will dominate the others. Therefore, piezoelectric actuators mounted to the incident plate will exert more effective control when the incident plate dominates the double panel system response; likewise piezoelectric actuators mounted to the radiating plate will exert more effective control when the radiating plate dominates the double panel system response. As was discussed previously, the sandwich board radiating plate double panel system does not exhibit such behavior.

It should be noted that the above analysis did not take the PZT control effort into account. This quantity is defined as the sum of the squares of the control voltages calculated in Eq. (34). As can

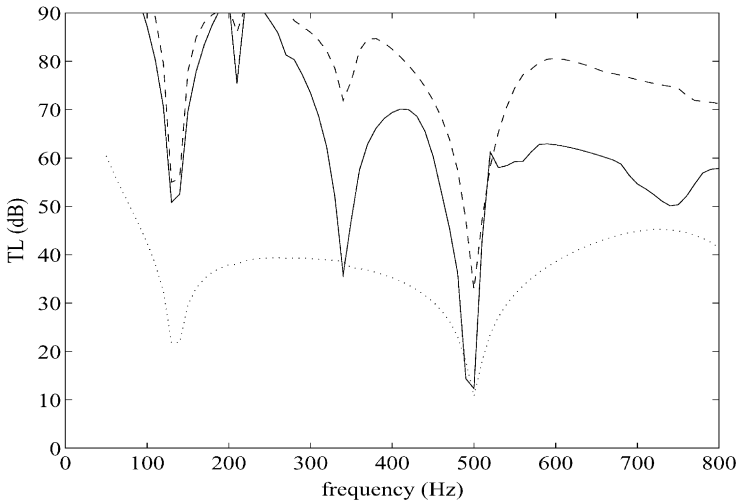

Fig. 8. Uncontrolled and controlled transmission loss for double panel system with PZTs located on incident and radiating plates (other parameters: oblique incident wave; sandwich board radiating plate): · · · ·, uncontrolled; ——, incident PZT; - - -, radiating PZT.

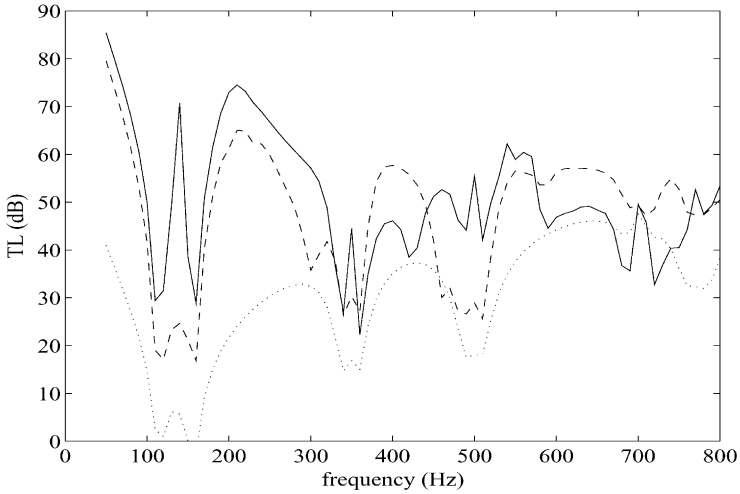

Fig. 9. Uncontrolled and controlled transmission loss for double panel system with PZTs located on incident and radiating plates (other parameters: normal incident wave; aluminum radiating plate): · · · ·, uncontrolled; ——, incident PZT; - - -, radiating PZT.

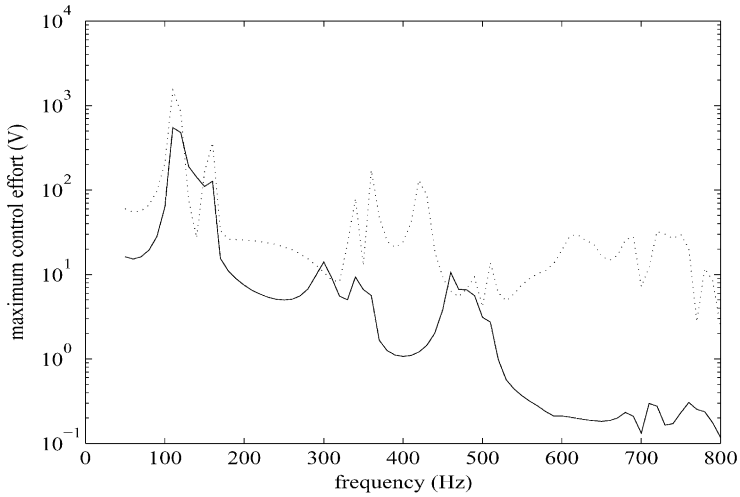

Fig. 10. Maximum control effort for PZTs located on incident and radiating plates of a double panel system (other parameters: normal incident wave; aluminum radiating plate): · · · ·, incident PZT; ——, radiating PZT.

be seen in Fig. 10, the control effort for the incident PZT case is significantly higher than the radiating PZT case. This again demonstrates that a direct coupling of the control actuators into the radiated acoustic field (i.e. PZTs located on the radiating plate) is beneficial. Taking the very large amount of increased control effort for the incident PZT case and the relatively small increase in frequency averaged transmission loss into account, placement of the PZT actuators on the incident plate would be a poor choice.

3.2.3. Effect of air cavity mass and stiffness on control performance

In this section, the influence of air cavity mass and stiffness on control performance is studied. The uncontrolled and controlled transmission loss for a double panel system cavity mass equal to air (M_s = air) and equal to twice that of air (M_s = 2air) is shown in Fig. 11. The double panel system was excited by a normal incident wave with PZT actuators located on an aluminum radiating plate. As can be seen, the additional mass of the air cavity has a small effect on control performance and the additional mass decreases the uncontrolled and controlled transmission loss. This effect also increases with frequency. This can be seen in the coupling terms of the double panel system equations in Eq. (4) where the mass term is multiplied by the square of the frequency.

The uncontrolled and controlled transmission loss for a double panel system cavity stiffness equal to air (K_s = air) and equal to twice that of air (K_s = 2air) is shown in Fig. 12. The double panel system was excited by a normal incident wave with PZT actuators located on an aluminum radiating plate. As can be seen, the additional stiffness of the air cavity has little effect on control performance, however the additional stiffness decreases uncontrolled and controlled transmission loss by approximately 6 dB. Note that the increased stiffness has little effect at the in-phase natural frequency (110 and 340 Hz). At these frequencies, the incident and radiating plates are vibrating in-phase with little relative motion between the plates and therefore the increased air cavity stiffness has little or no effect. This can be seen in the double panel system equations in Eq. (1) where the air cavity stiffness is written as a function of the difference of the incident and radiating plate flexural motion. However, the increased stiffness has the effect of increasing the out-of-phase resonant frequencies. For example, the out-of-phase fundamental is increased from 156 Hz to approximately 190 Hz as seen in Fig. 12.

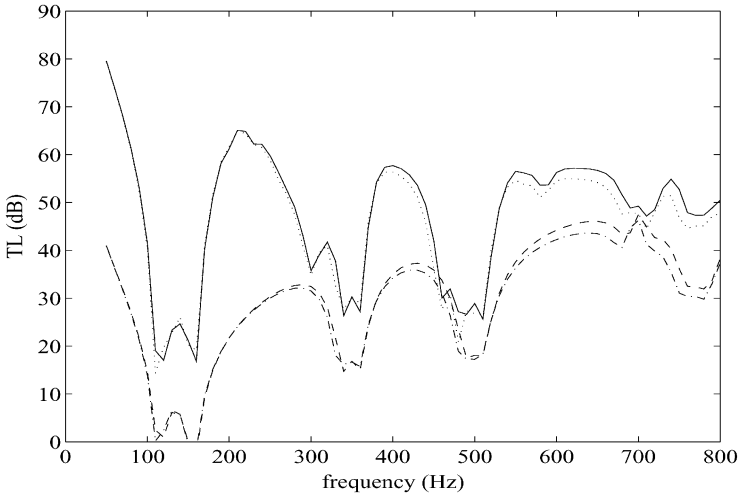

Fig. 11. Uncontrolled and controlled transmission loss for double panel system with cavity mass equal to air (M_s = air) and double air mass (M_s = 2air) (other parameters: normal incident wave; PZTs located on aluminum radiating plate): - - -, uncontrolled baseline; - · -, uncontrolled 2 times mass; ——, controlled baseline; · · · ·, controlled 2 times mass.

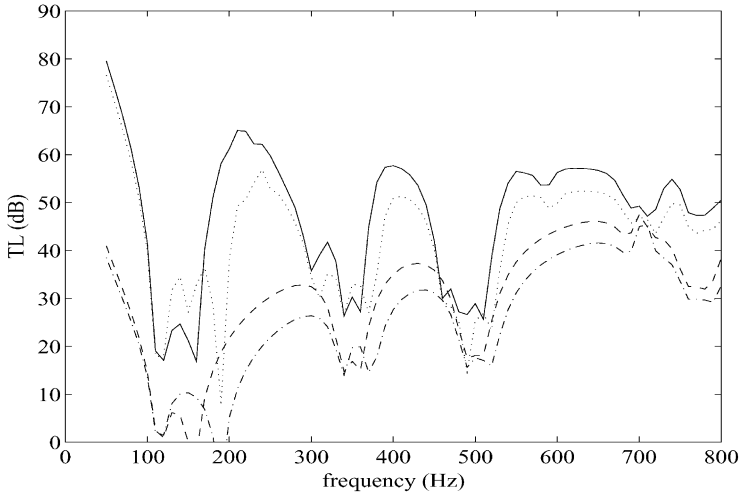

Fig. 12. Uncontrolled and controlled transmission loss for double panel system with cavity stiffness equal to air (K_s = air) and double air stiffness (K_s = 2air) (other parameters: normal incident wave; PZTs located on aluminum radiating plate): - - -, uncontrolled baseline; - · -, uncontrolled 2 times stiffness; ——, controlled baseline; · · · ·, controlled 2 times stiffness.

4. Concluding discussion

An analytical model for studying the ASAC of double panel systems has been developed. This double panel system model approximates the noise transmission path from the exterior of an aircraft fuselage to the interior noise field. A comparison of theoretical and experimental uncontrolled transmission loss verified that the double panel system model generally describes the system behavior.

A parametric study of the ASAC of double panel system was then performed. A double panel system with a stiff radiating plate exhibits a decreased coupling of the incident and radiating plates and a lower modal density, which results in increased controlled transmission loss. The increased stiffness also leads to a lower double panel system response and increased uncontrolled transmission loss. A stiffer radiating plate was also seen to decrease the control effort required due to better impedance matching between the PZT and the radiating plate. Taking the control effort into account, piezoelectric (PZT) control actuators should be mounted on the radiating plate of a double panel system, which can couple into the radiating acoustic field better than actuators mounted on the incident plate. Doubling the air cavity mass has little effect on control performance, however uncontrolled TL is slightly reduced at higher frequencies (>400 Hz). Doubling the air cavity stiffness increases the coupling between the incident and radiating plates resulting in decreased uncontrolled TL and slightly better control performance for PZT actuators mounted on the incident plate.

This investigation has shown the potential for applying Active Structural Acoustic Control to reduce the interior noise of an aircraft by taking advantage of control actuator location and double panel system stiffness. Future investigations will investigate the amount of local versus

global control that is achieved by applying the piezoelectric actuators to the interior trim and the incorporation of novel control algorithms.

Acknowledgements

The authors acknowledge the support of this work by the Structural Acoustics Branch of NASA Langley Research Center with Dr. Harold Lester as Technical Monitor.

Appendix A. Nomenclature

α_x, α_y	$m\pi$/lx and $n\pi$/y, respectively
ε_{pe}	PZT constant
ω_{mn}	mnth natural frequency
ρ	density
v	the Poisson ratio
ω	frequency (rad/s)
Θ	transfer function
θ	polar co-ordinate
ϕ	polar co-ordinate
Π	acoustic power
Ψ	piezoelectric modal coupling coefficient
τ	transmission coefficient
η	damping coefficient
∇	gradient
C	damping coefficient
C_o	PZT constant
c	speed of sound in medium
D	Stiffness of structure
d_{31}	piezoelectric strain constant
E	modulus of elasticity
h	thickness of structure
I	acoustic intensity
j	square root of (-1)
K	air spring coefficient
k	acoustic wavenumber
k_s	structural wavenumber
l_x, l_y	length of structure in x and y directions, respectively
m	mass density per unit area of the structure
N	number of frequency bins
P	acoustic pressure amplitude
p	acoustic pressure
p_{mn}	modally decomposed pressure

r	radius (polar co-ordinate)
TL	transmission loss
t	time
V	voltage
W	modal response of structure
w	flexural response of structure
x, y	Cartesian co-ordinates
Y	integration of far field radiation terms

Subscripts

b	blocked
i	incident
m, n	modal indices
r	radiating
s	air cavity
x, y	x and y direction, respectively

Superscripts

c	control
d	disturbance
i	incident
r	radiating
t	total

References

[1] J.P. Carneal, C.R. Fuller, Active structural acoustic control of noise transmission through double panel systems, *American Institute of Aeronautics and Astronautics Journal* 33 (4) (1995) 618–623.
[2] P.A. Nelson, S.J. Elliot, *Active Control of Sound*, Academic Press, New York, 1992.
[3] R. Vaicaitis, Study of noise transmission through double wall aircraft windows, NASA Contractor Report 172182, 1983.
[4] A. Leissa, *Vibrations of Plates*, Acoustical Society of America, 1993.
[5] A. Berry, J.L. Guyander, J. Nicholas, A general formulation for the sound radiation from rectangular, baffled plates with arbitrary boundary conditions, *Journal of the Acoustical Society of America* 88 (6) (1990) 2792–2802.
[6] L.A. Roussos, Noise transmission loss of a rectangular plate in an infinite baffle, NASA Technical Paper 239, 1985.
[7] A.D. Pierce, *Acoustics: An Introduction to its Physical Principles and Applications*, McGraw-Hill, New York, 1980.
[8] F. Fahy, *Sound and Structural Vibration*, Academic Press, New York, 1985.
[9] E.K. Dimitriadis, C.R. Fuller, Investigation on active control of sound radiation from a panel using piezoelectric actuators, *American Institute of Aeronautics and Astronautics Joumal* 29 (11) (1991) 1771–1777.
[10] T. Song, The Optimal Design of Transducers for Active Control of Multiple-frequency Structural Sound Radiation, Ph.D. Dissertation, Virginia Polytechnic Institute and State University, 1995.
[11] C.R. Fuller, P.A. Nelson, S.J. Elliot, *Active Control of Vibration*, Academic Press, London, 1996.